PAPER

Vortex dynamics and second magnetization peak in the iron-pnictide superconductor $Ca_{0.82}La_{0.18}Fe_{0.96}Ni_{0.04}As_2$

IOP Publishing

Superconductor Science and Technology

Supercond. Sci. Technol. **34** (2021) 115010 (8pp)

https://doi.org/10.1088/1361-6668/ac2556

Vortex dynamics and second magnetization peak in the iron-pnictide superconductor $Ca_{0.82}La_{0.18}Fe_{0.96}Ni_{0.04}As_2$

I F Llovo[1], D Sóñora[1], J Mosqueira[1], S Salem-Sugui Jr[2,*], Shyam Sundar[2,*], A D Alvarenga[3], T Xie[4], C Liu[4], S-L Li[4,5] and H-Q Luo[4,5]

[1] QMatterPhotonics Research Group, Departamento de Física de Partículas, Universidade de Santiago de Compostela, Santiago de Compostela E-15782, Spain
[2] Instituto de Fisica, Universidade Federal do Rio de Janeiro, 21941-972 Rio de Janeiro, RJ, Brazil
[3] Instituto Nacional de Metrologia Qualidade e Tecnologia, 25250-020 Duque de Caxias, RJ, Brazil
[4] Beijing National Laboratory for Condensed Matter Physics, Institute of Physics, Chinese Academy of Sciences, Beijing 100190, People's Republic of China
[5] Songshan Lake Materials Laboratory, Dongguan, Guangdong 523808, People's Republic of China

E-mail: said@if.ufrj.br and shyam.phy@gmail.com

Received 1 July 2021, revised 23 August 2021
Accepted for publication 9 September 2021
Published 29 September 2021

Abstract

We report the studies of detailed magnetic relaxation and isothermal magnetization measurements in the vortex state of the 112-type iron-pnictide $Ca_{0.82}La_{0.18}Fe_{0.96}Ni_{0.04}As_2$ superconductor with $T_c \sim 22$ K. In the isothermal $M(H)$, a well defined second magnetization peak (SMP) feature is observed in the entire temperature range below T_c for measurements with $H \parallel c$-axis. However, for $H \parallel ab$-planes, the SMP feature is suppressed at low temperatures, which might be due to 2D Josephson vortices forming at low temperatures and high magnetic fields in such an anisotropic system. A rigorous analysis considering the magnetic relaxation data for $H \parallel c$-axis suggests an elastic to plastic pinning crossover across H_p, which also seems accompanied with a possible phase transition in vortex lattice near H_p. Moreover, point disorder and surface defects are likely to be the dominant sources of pinning, which contribute to the δl-type of pinning in the sample. A high J_c, in access of 10^5 A cm^{-2} observed could potentially make this material technologically important.

Keywords: iron-pnictide superconductors, vortex dynamics, critical current density, vortex pinning, second magnetization peak

(Some figures may appear in colour only in the online journal)

1. Introduction

Vortex physics in iron-pnictide superconductors is of a great importance for many future technological advancements [1] as well as for the understanding of various exciting phases of vortex matter [2]. Among the various interesting phenomenon observed in the vortex state of type-II superconductors, the second magnetization peak (SMP) phenomenon in the isothermal magnetization curves is one of them. Such phenomenon is ubiquitous in various low-T_c conventional [3, 4] as well as in high-T_c unconventional superconductors [5, 6] and even in superconductors exhibiting multiple superconducting gaps, such as MgB_2 [4]. Also, the SMP has been investigated in nearly all families of iron-pnictide superconductors for magnetic field directions parallel and perpendicular to

* Authors to whom any correspondence should be addressed.

the crystal ab-plane [7] (and references therein), its occurrence has not been observed in some pnictide crystals even with $H \parallel c$-axis, as for instance in overdoped Ba-KFe_2As_2 [8], in (Li-Fe)OHFeSe [9], in La-doped $CaFe_2As_2$ [10] and in $La_{0.34}Na_{0.66}Fe_2As_2$ [11]. The importance of the SMP appearing on isothermal magnetization curves relies on its direct association with the peak effect appearing in the magnetic field dependence of critical current density, $J_c(H)$ [12], which is of technological importance.

Despite it being observed in many superconductors, the mechanism responsible for the SMP is not totally understood and it appears to be material dependent [13]. For this reason the SMP has been studied in many different systems, usually by means of the vortex dynamics. Since the discovery of iron-pnictide superconductors [14] the SMP has been observed in many of these systems and explained in terms of a pinning-crossover as observed for Ba(Fe-Co)$_2$As$_2$, (Ba-K)Fe_2As_2, Ba(Fe-Ni)$_2$As$_2$, Ca(Fe-Co)As and (Ca-La)(Fe-Co)As_2 [15–22], in terms of a phase transition in the vortex lattice as observed for Ba(Fe-Co)$_2$As$_2$, LiFeAs, and $BaFe_2$(As-P)$_2$ [23–26], and also in terms of an order-disorder transition in some compounds [27–29]. It is to note that all the systems mentioned above share a similar layered crystal structure which consists of a spacer layer in-between of FeAs superconducting layers. However, the crystal structure in the 112 family has an additional spacer layer which leads to the enhanced spacing between FeAs superconducting layers [30]. This contributes to the anisotropic superconducting properties in 112 family [31–33]. Since, the observed SMP in moderate anisotropic 1111-system is found to be due to the 3D order to 2D disorder phase transition [34, 35], it is interesting to find if a sample of 112-system with similar anisotropy as 1111-system has the same origin of SMP.

Here, we investigate the SMP and pinning behavior in a single crystal of the 112 type pnictide $Ca_{0.82}La_{0.18}Fe_{0.96}Ni_{0.04}As_2$ superconductor with superconducting temperature transition $T_c \sim 22$ K [36] and moderate anisotropy [33]. A well pronounced SMP is observed in all isothermal $M(H)$ curves obtained with $H \parallel c$-axis even for temperatures very close to T_c ($T = 20$ K), and also for $H \parallel ab$-planes but only for temperatures above 14 K. As the SMP has been observed for $H \parallel c$-axis and $H \parallel ab$-planes in most of the pnictide superconductors [37–39], its absence for $H \parallel ab$-planes at lower temperatures (below 7.5 K) might be related to the anisotropic nature of the sample [33] that might leads to the possible emergence of two dimensional Josephson vortices at low temperatures and high magnetic fields [6, 40].

In order to study the possible origin of the SMP observed for H||c-axis in our sample, extensive magnetic relaxation measurements were performed. For $H \parallel ab$-planes, magnetic relaxation data were within the noise level of the measurements, which prevented us from studying the vortex dynamics for this direction. The behaviour of the relaxation rate, $R = \mathrm{dln}M/\mathrm{dln(time)}$, with field and temperature, as well as the dependence of the activation energy, $U_0 = -T/R$ [41] with the critical current [42] and of $U(M)$ with $M - M_{\mathrm{eq}}$ [43–45], allowed us to study the vortex dynamics in the magnetic phase diagram of the system, and also to address the underlying mechanism for SMP. A crossover from collective (elastic) to plastic pinning has been observed across SMP, which is also accompanied with a possible phase transition in vortex lattice near H_p. Moreover, point disorder and surface defects seem to be the possible sources of vortex pinning in the sample. Self-field critical current density for $H \parallel c$-axis achieves $J_c = 7 \times 10^5$ A cm^{-2} at $T = 2$ K.

2. Experimental details

The $Ca_{0.82}La_{0.18}Fe_{0.96}Ni_{0.04}As_2$ single crystal used in this work was grown by a self-flux method as used in many other iron-based superconductors. A small crystal of mass, 0.306 mg with a roughly triangular platelet shape of surface area $S = 0.65$ mm^2 and thickness $t = 83.4$ μm (as determined from the density $= 5.64$ g cm^{-3}, calculated from the lattice parameters) was used in this study. A thorough description of the growth procedure can be seen in [36]. Details of the characterization by energy-dispersive x-ray spectroscopy (EDX) and x-ray diffraction can be seen in [33] (crystal 11 of that reference). Let us just mention that it presents an excellent stoichiometric quality, with $x = 0.176(3)$ and $y = 0.045(3)$, and its diffraction pattern shows no spurious diffraction peaks, the c-axis lattice parameter being 10.348(1) Å.

The magnetization M measurements were performed with a magnetic-properties measurement system (Quantum Design, model MPMS-XL) with magnetic fields up to 7 T applied both parallel and perpendicular to the crystal's *ab* layers. For this purpose, a quartz tube was used as sample holder, to which the crystal was glued with GE varnish. In the case of $H \parallel c$, the crystal was glued to a $\sim$0.3 mm-wide slit, perpendicular to the quartz tube axis. Two plastic rods at the sample holder ends ensured an alignment of about 0.1°. $M(H)$ hysteresis curves were measured for both $H \parallel ab$ and $H \parallel c$, by using the MPMS's *hysteresis* magnetic field charging mode. $M(t)$ relaxation curves were measured for $H \parallel c$ only (for $H \parallel ab$ the M variation was of the order of the noise level).

3. Results and discussion

Figure 1 shows selected isothermal magnetization, $M(H)$, curves as obtained for $H \parallel c$-axis (a) and $H \parallel ab$- planes (b). All M(H) curves shown in figure 1 are symmetric with respect to the magnetic field axis which reflects the dominant bulk pinning of the samples. The main information that can be extracted from these figures is that a pronounced second magnetization peak is observed for all $M(H)$ curves obtained with $H \parallel c$-axis. However, for $H \parallel ab$-planes the SMP is only observed in the temperature region above 7.5 K. As shown in figure 1(b), the $M(H)$ curves below 14 K would show a SMP developing at increasingly higher fields at low temperatures, although below 7.5 K both branches of the $M(H)$ curves decreases monotonically. The disappearance of the SMP for $H \parallel ab$-planes below 7.5 K is possibly related to the moderate anisotropy of the studied system, which may cause it to enter in a two dimensional regime for higher fields [33]. We conjecture that the possible emergence of the Josephson vortices

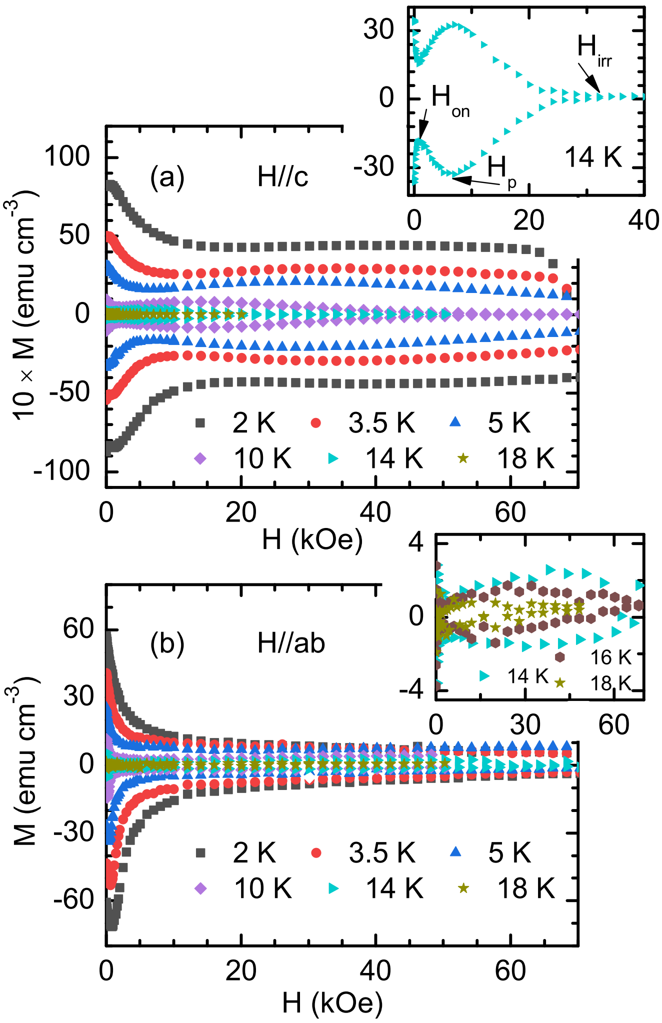

Figure 1. (a) Isothermal magnetic field dependence of the magnetization, $M(H)$, at selected temperatures well below T_c for $H \parallel c$. In inset, the characteristic fields H_{on}, H_{p} and H_{irr} are well defined for $M(H)$ measured at $T = 14$ K. (b) Isothermal $M(H)$ at selected temperatures for $H \parallel ab$. Inset shows the clear signature of SMP in isothermal $M(H)$ measured at 14 K, 16 K and 18 K.

within the 2D regime would prevent the SMP to develop at low temperatures (below 7.5 K) due to the weaker pinning of the Josephson vortices than Abrikosov vortices [6, 46]. The curves of figure 1(a) allow to extract the characteristic fields H_{on}, H_{p} and H_{irr} which are respectively the onset field of the SMP, the peak field, and the irreversible field. H_{irr} was selected as the magnetic field at which the hysteresis amplitude becomes of the order of magnitude of the experimental noise. An example of H_{irr} obtained by this criterion is shown in the inset of figure 1(a). We observe that the SMP develops even for temperatures very close to T_c for $H \parallel c$-axis direction. It is worth mentioning that the onset field H_{on} and peak field, H_{p} associated to the SMP for $H \parallel c$-axis are well defined in all isothermal $M(H)$ curves even at $T = 2$ K.

In order to study the possible origin of the second magnetization peak in the sample, magnetic relaxation measurements were performed as a function of field for selected isothermal $M(H)$ curves, and as a function of temperature for selected applied magnetic fields. The study was only conducted for $H \parallel c$, as values of the magnetic moment during relaxation were within the noise level observed for $H \parallel ab$- planes measurements. Magnetic relaxation curves were obtained for span times of about 80 minutes, and plots of ln$M$ vs ln(time) produced the usual linear curves from which the values of the relaxation rate $R = \mathrm{dln}M/\mathrm{dln(time)}$ were extracted. Figure 2 shows plots of $M(H)$ curves obtained at $T = 10$ K and 12 K, along with the respective relaxation rate curves obtained over each $M(H)$ curve from fields going from below H_{on} up to above H_{p}. A change in the curvature of R vs. H can be observed for fields in the vicinity of H_{p}, the peak field, which might suggests a change in the pinning behaviour occurring near H_{p}. Moreover, a change in the curvature of each R vs. H near H_{on} is associated to crossover of the single vortex pinning to collective vortex pinning [16]. Similar peaks in the R vs. H curves, appearing between H_{on} and H_{p} have also been observed previously in other iron-pnictide superconductors [16, 18] which have been attributed to a precursor phenomenon that leads to a SMP at higher fields [47].

To check for the change in curvature observed in the curves of figures 2(a) and (b) for H near H_{p}, magnetic relaxation measurements as a function of temperature for $H = 10$, 15, and 20 kOe were performed. Figure 2(c) shows the resulting R vs T curves where a clear change in the behaviour of R is observed near T_{cr} (marked with an arrow). Later in the paper, it will be shown in the H-T phase diagram that the T_{cr} obtained for each field is well matched with H_{p} vs. T.

As the R vs. T, and R vs. H plots suggest a possible pinning crossover near H_{p}, it would be interesting to see the behaviour of the activation pinning energy, $-T/R$ against $1/J_c$, where J_c is the critical current density. Figure 3(a) shows selected curves of the magnetic field dependence of the critical current density, $J_c(H)$ for $H \parallel c$-axis as calculated using Bean's critical-state model [48]. An expression for a triangular platelet with magnetic field parallel to c-axis was used to estimate the J_c in the sample [49], $J_c(T,H) = \frac{15\Delta M(T,H)}{\sqrt{s^{-1}(s-a)(s-b)(s-c)}}$, where $a \approx 1.25$ mm, $b \approx 1.10$ mm, and $c \approx 1.37$ mm are the sides of the triangle, $s = (a+b+c)/2$ is its semiperimeter, and $\Delta M(T,H)$ is the magnetization hysteresis. A peak, associated to the SMP in $M(H)$, is clearly visible for each $J_c(H)$ curve shown in figure 3(a).

According to the collective pinning theory, [42] the activation energy $U \sim (1/J_c)^{\mu}$, where μ is a critical exponent. From this critical exponent, information about how the vortices are collectively pinned can be obtained. For instance, $\mu = 1/7$ corresponds to single vortex, $\mu = 3/2$ to small bundles of vortices and $\mu = 7/9$ to large bundles. Figure 3(b) shows two distinct behaviours occurring for all isofield curves where for lower values of the inverse critical current density, which corresponds to the region below H_{p}, the exponent $\mu = 1.07$ and 0.98 for $H = 10$ kOe and 15 kOe respectively and $\mu = 0.63$ for $H = 20$ kOe. Such values of μ are in agreement with a vortex lattice collectively pinned as small bundles and large bundles. The region corresponding to larger values of the inverse critical current density, which corresponds to the region above H_{p},

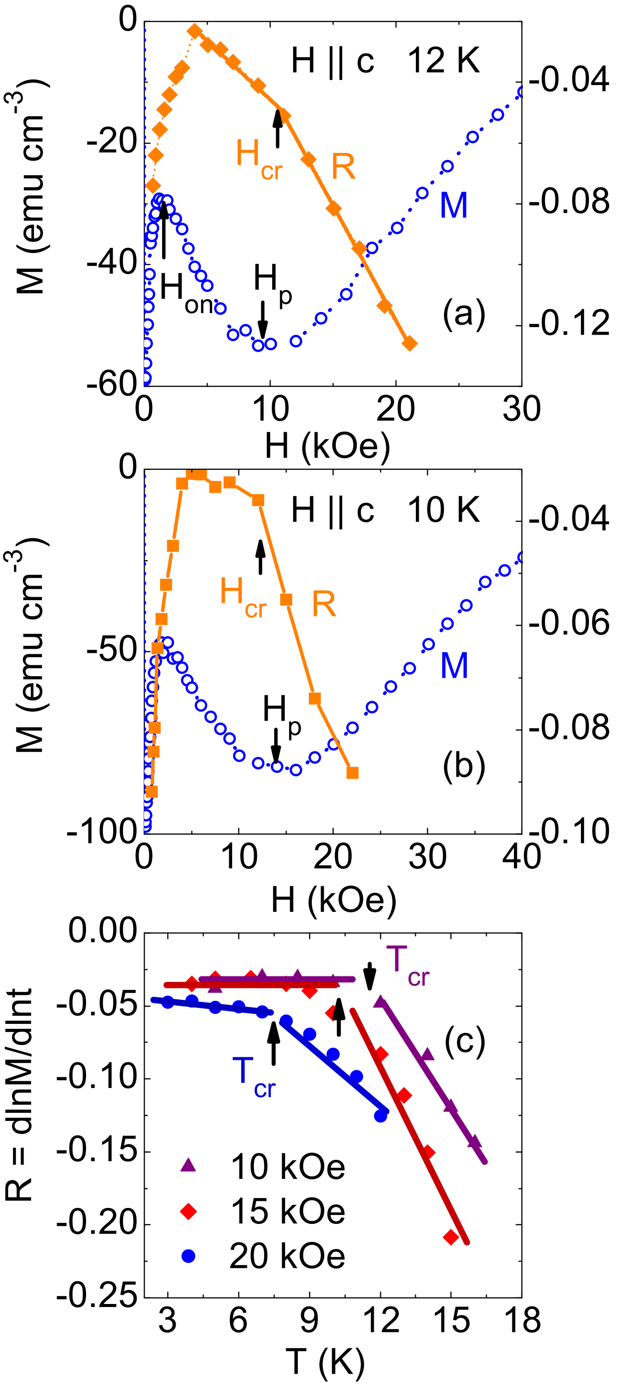

Figure 2. ((a) and (b)) Isothermal magnetic field dependence of the magnetization, $M(H)$, measured at $T = 12$ K and 10 K, in the increasing magnetic field branch and the obtained relaxation rates, R, at fixed magnetic fields between H_{on} and H_{p} for respective $M(H)$. H_{cr} indicates the change in slope in $R(H)$ which matches well with H_{p}. (c) Relaxation rate as a function of temperature, $R(T)$, for $H =$ 10 kOe, 15 kOe and 20 kOe. Arrows indicate, T_{cr}, the temperature where slop changes in each $R(T)$.

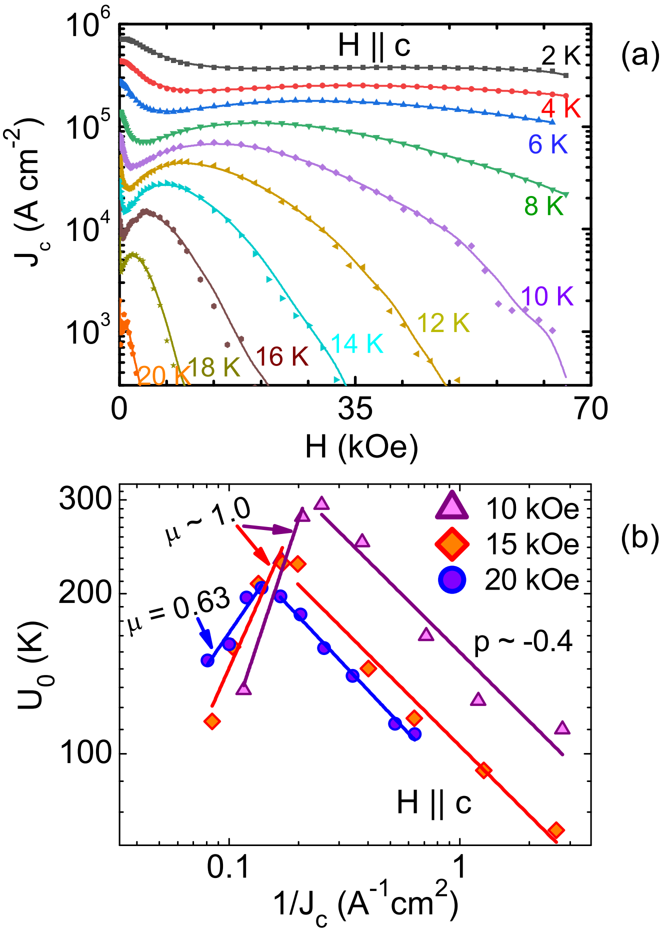

Figure 3. (a) Critical current density as a function of magnetic field, $J_c(H)$ obtained using Bean's critical state model [48] for $H \parallel c$. Solid lines are guide to eyes. (b) Activation energy, $U_0 = \mathrm{T/R}$, as a function of inverse critical current density, $1/J_c$, for $H = 10$ kOe, 15 kOe, and 20 kOe. The exponents μ and p found for each curve indicates an elastic pinning to plastic pinning crossover across SMP.

possesses a negative exponent which can not be explained in terms of the collective pinning theory. Such a region with a negative exponent [17, 21] has been associated to plasticity of the vortex lattice, where the characteristic exponent is $p = -0.5$. As it can be observed in figure 3(b), the exponent p obtained for the three fields data is $p \sim$-0.4 ($p = -0.4$ for $H =$ 10, $p = -0.37$ for 15 kOe and $p = -0.46$ for $H = 20$ kOe) which agrees with the plastic exponent $p = -0.5$. Figure 4 suggests that the mechanism responsible for the second magnetization peak appearing in $M(H)$ curves in our sample is a crossover from collective to plastic pinning occurring as the SMP develops. It should be mentioned that such behavior, separating a low J_c region from a higher J_c region in U_0 vs. $1/J_c$ isofield curves, has also been observed previously in systems which do not exhibit the second magnetization peak [11]. To further study this change in behavior, a more rigorous analysis of the activation energy was performed, as first presented in [45].

The characteristic fields, H_{on}, H_{p} and H_{irr} obtained from the isothermal $M(H)$ curves for $H \parallel c$-axis are plotted as a function of temperature in the $H-T$ phase diagram, shown in figure 4. Contrary to the H_{on} line, the temperature dependence of H_{p} and H_{irr} follow $\sim (1-(T/T_c))^n$ behavior, where, $n = 2$, 1.3 are obtained for H_{p} and H_{irr} lines respectively. A similar temperature dependence of the irreversibility line was also observed in [50]. It is interesting to note that at low T, the H_{on} and H_{p}

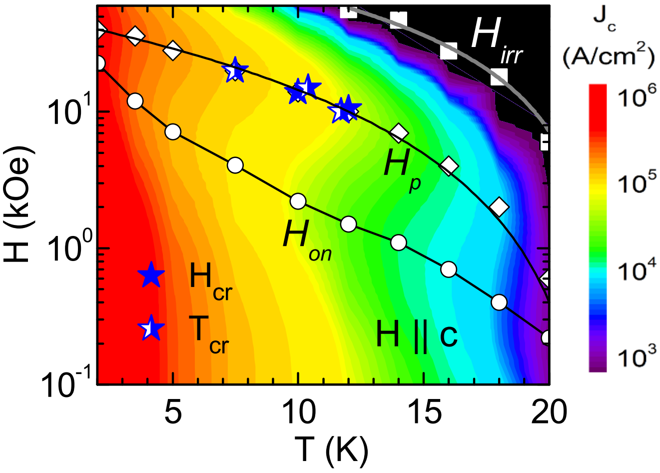

Figure 4. An H-T phase diagram representing the characteristic fields, H_{on}, H_p and H_{irr}. Solid lines in H_{irr} and H_p are fit to the data as explained in the text. H_{cr} and T_{cr} are field and temperature marked in figure 2. Solid line in H_{on} is guide to the eyes. The critical current density as a function of magnetic field at different temperatures is plotted in a contour plot.

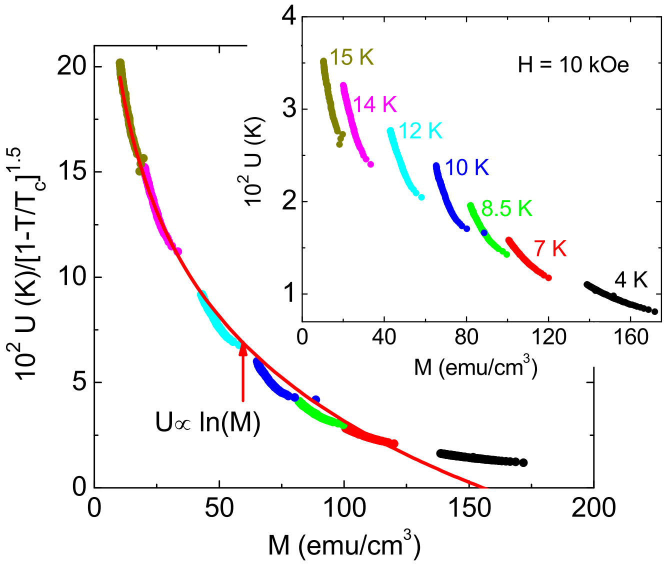

Figure 5. $U/g(T/T_c)$ vs. M scaled plot obtained for $H = 10$ kOe using Maley's criterion explained in the text. Solid line shows the $\ln(M)$ dependence of scaled curve. Inset shows the $U(M)$ without scaling using $g(T/Tc)$ function.

follow relatively opposite curvatures with temperature, which may lead to the merging of H_p and H_{on} lines at temperatures below 2 K. A merging of the H_{on} line with the H_p line at high fields would imply the disappearance of the SMP, which in the present case of a highly anisotropic system, could be associated to a possible field-induced crossover to a two dimensional vortex system. It should be mentioned that the vortex physics associated to the H_{on} and H_p are different in nature, where, H_{on} is reported to be associated to a crossover from single vortex-pinning to a collective vortex-pinning regime [17, 19, 45]. This supports a change in pinning strength from weak to strong across H_{on} as reported in reference [51]. On the other hand, different mechanisms have been reported to be responsible for the SMP at H_p in different systems, as discussed in the introduction. The origin of the SMP in present sample is discussed in the later part of the paper. We also plot in the phase diagram the corresponding H_{cr} and T_{cr} values of the kinks observed in R vs. H and R vs. T plots respectively. It is interesting to note that the H_{cr} and T_{cr} points in the $H-T$ phase diagram lie almost perfectly on the H_p line. This fact, despite evidencing a change in the pinning mechanism, as discussed above, may also be related to a possible vortex lattice phase transition taking place as the second magnetization peak develops [5, 52], which deserves further investigation. Moreover, a contour plot of J_c obtained at various temperatures below T_c in the magnetic field range 0–7 T is also shown in figure 4, to track the H_{on}, H_p and H_{irr} with the changes in $J_c(H,T)$.

The activation energy, $U(M)$, was obtained following an approach developed by Maley *et al* [43, 44] assuming that the isofield $U(M)$ curves measured at different temperatures should be a smooth function of $M-M_{eq}$, where M_{eq} is the equilibrium magnetization. It should be mentioned that for our system $M-M_{eq}\approx M$. In this approach, $U(M)=-T\ln(dM/dt)+CT$, where C is an intrinsic constant. $U(M)$ is then calculated from the isofield relaxation curves obtained for several temperatures and plotted as a function of M. The appropriate constant C for the system defines the smooth curve. But as pointed out in [44], for most systems the smooth curve is only obtained by dividing $U(M)$ by a scaling function $g(T/T_c)$ which carries the behavior of the coherence length $\xi(T)$. Figure 5 shows a plot of $U/(1-T/T_c)^{3/2}$ vs. M for $H = 10$ kOe exhibiting a smooth behavior with M, which was obtained for $C = 15$. Similar curves with the same constant C were obtained for $H = 15$ and 20 kOe (not shown here for brevity). With the value of $C = 15$ we can calculate $U(M)$ from the isofield magnetic relaxations obtained on the isothermic $M(H)$ curves for fields below and above the H_p. Figure 6(a) shows the $U(M)$ curves obtained for isothermal $M(H)$ at 12 K where a clear change in the behavior of $U(M)$ is observed as H_p is crossed. To check for a possible pinning crossover across H_p, we exploited an expression from the collective pinning theory, $U(B,J)=B^{\nu}J^{-\epsilon}\approx H^{\nu}M^{-\epsilon}$, where, ν and ε are exponents for specific pinning. Figure 6(b) shows plots of selected $U(M)$ curves of figure 6(a) after being scaled by H^{ν}, as in [45]. For H below and above H_p, the scaling was obtained for $\nu = 0.5$ and -0.5 respectively. A positive value of exponent ν supports the collective pinning for $H < H_p$ [42, 45], whereas a negative ν exponent for fields above H_p supports plastic pinning. Although, the expected values of ν are 1 and -0.5 for collective and plastic pinning respectively, exponent ν smaller than 1, associated to collective pinning, have also been observed in other systems [6, 17, 18]. The inset of figure 6(b) shows the corresponding $M(H)$ at 12 K evidencing H_p. The plots of figure 6(b) clearly demonstrate that the mechanism explaining the second magnetization peak in our sample is a crossover from collective to plastic pinning occurring as the peak field H_p is crossed. As discussed in the

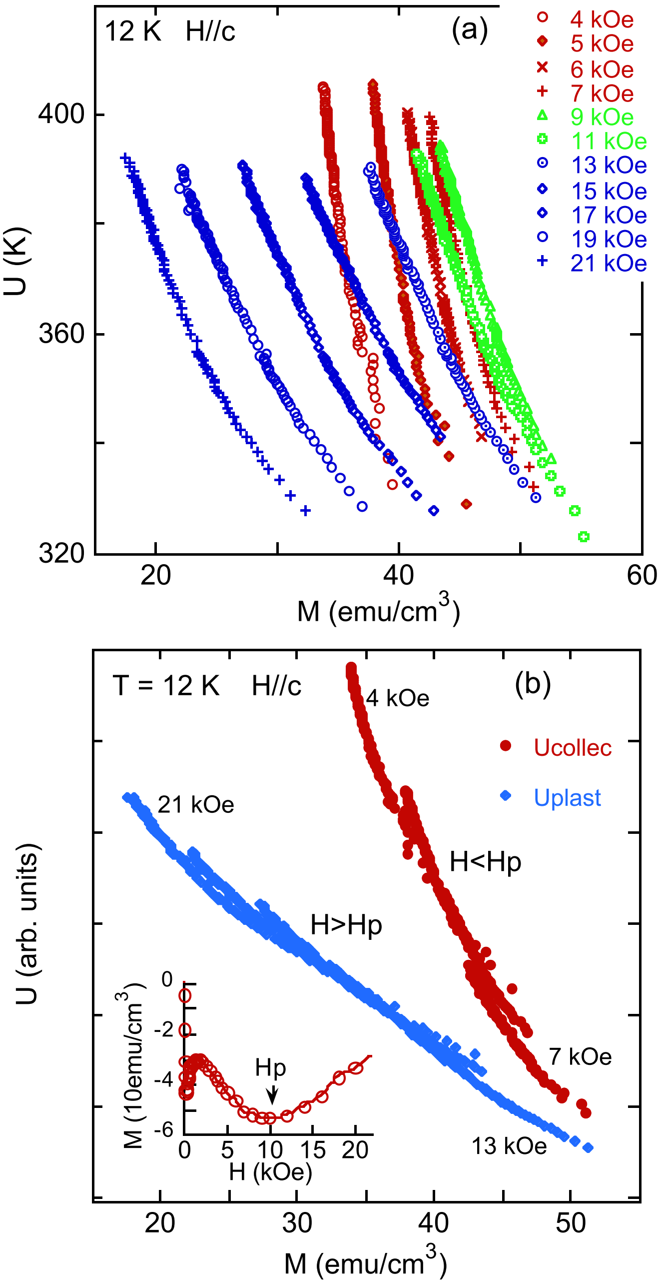

Figure 6. (a) Activation energy, U, vs. magnetization, M, for different magnetic fields above and below the H_p at $T = 12$ K. (b) Scaled U curves using collective pinning theory show elastic pining for $H < H_p$ and plastic pinning for $H > H_p$. Inset shows the initial branch of $M(H)$ measured at $T = 12$ K for $H \parallel c$-axis.

previous paragraph, there is also a possibility of vortex lattice phase transition below H_p. Such change in vortex lattice near H_p may creates an energetically favorable scenario for the plastic pinning at fields above H_p. Similar behavior has also been observed in the case of Co-doped 122 iron pnictide superconductor, where a a vortex lattice phase transition below H_p accompany the collective to plastic creep crossover across H_p [16, 23, 53]. Moreover, Kopeliansky *et al* [23] also stated that such a crossover (collective-plastic) in vortex dynamics may accompany a thermodynamic phase transition in vortex lattice, as seen previously in case of YBCO [45, 54]. However, any direct observation of vortex lattice phase transition below H_p and its correlation with SMP is yet to be confirmed in iron pnictide superconductors.

Figure 7(a) shows a plot of the so called remanent critical current density normalized by its value extrapolated to $T = 0$, $J_c(T)/J_c(0)$ against temperature for $H \parallel c$-axis. The remanent critical current corresponds to the critical current at zero field extracted from the Bean's model, where ΔM is obtained by subtracting the magnetization for $H = 0$ belonging to the decreasing field branch from the magnetization curve for $H = 0$ belonging to the increasing field branch after cycling the correspondent isotherm $M(H)$ in negative magnetic fields. For comparison, figure 7(a) also shows the values obtained from a model developed in [55] which considers two possible pinning of the type δl, for which $J_c(T)/J_c(0) \sim (1-t^2)^{5/2}(1+t^2)^{-1/2}$, and δT_c, for which $J_c(T)/J_c(0) \sim (1-t^2)^{7/6}(1+t^2)^{5/6}$, where $t = T/T_c$. As observed in other pnictides [17] and references therein, the dominant pinning in our sample follows neither of the above two behaviors considered in [55]. However, such behavior of $J_c(T)$ may be explained considering the weak and strong pinning at low and high magnetic fields respectively, as shown in case of $FeSe_{0.5}Te_{0.5}$ superconductor [56].

Figure 7(b) shows a plot of the normalized pinning force density, $F_p(H)/F_{pmax}$, as a function of the reduced field $h = H/H_{irr}$, for several temperatures. The pinning force density is obtained using expression, $F_p = H \times J_c$. The scaling of the different isothermal $F_p(H)/F_{pmax}$ curves with $h = H/H_{irr}$ is a powerful tool [57, 58] commonly used in new materials to identify the dominant pinning acting within certain temperature regions [59]. The importance of this plot also relies on the identification of the magnetic field region, h_{max}, where the pinning force presents its maximum, which might be important for application purposes [57, 58]. As shown in figure 7(b), all curves collapse in one, with a very clear maximum appearing for $H/H_{irr} = 0.27$. The solid curve in this figure is a best fit to the well known Dew-Hughes expression, $F_p(H)/F_{pmax} \sim h^p(1-h)^q$, where values of p and q are associated to the characteristic types of pinning explained in the model [57]. The best fit shown in figure 7(b) was obtained with $p = 2$ and $q = 5.5$ where $h_{max} = p/(p+q) \sim 0.27$, which is consistent with the h_{max} observed from data. It is important to mention that in Dew-Hughes model [57, 58], δl pinning due to point disorder expects $p = 1$ and $q = 2$, with $h_{max} = 0.33$. Therefore, in our case, $h_{max} = 0.27$ indicates the pinning due to point disorder. However, higher values of p and q and slightly lower h_{max} than what is ideally expected for Dew-Hughes model, suggests additional pinning at play, likely due to the surface defects. Similar results have been observed in other iron pnictide superconductors as reported in [18, 60–62]. Moreover, according to Dew-Hughes model [57], $h_{max} < 0.5$ indicates a δl pinning, while $h_{max} > 0.5$ suggests δT_c pinning, therefore, $h_{max} = 0.27$ in present case is suggestive of δl pinning. In addition, more than one pinning centers at play may lead to the deviation from the δl pinning model, as observed in figure 7(a).

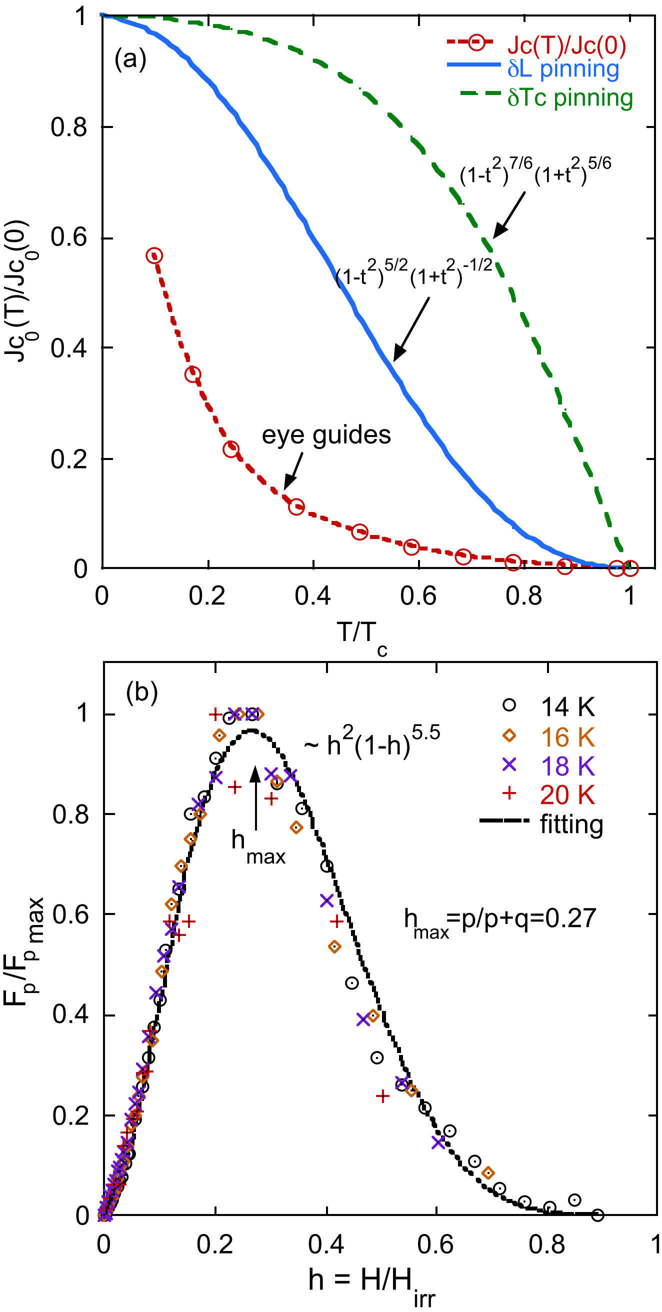

Figure 7. (a) Normalized critical current density, $J_c(T)/J_c(0)$ as a function of reduced temperature, $t = T/T_c$ from experimental data. Solid lines represents the δl and δT_c pinning using models in [55]. (b) Normalized pinning force density, $F_p(H)/F_{\rm pmax}$, as a function of the reduced field, $h = H/H_{\rm irr}$ for different temperatures. The solid line is the fitting of scaled curves using the expression, $F_{\rm p}(H)/F_{\rm pmax} \sim h^p(1-h)^q$, where, p and q are fitting parameters [57]. Details of the fit are given in the main text.

4. Conclusions

In conclusion, we investigated the second magnetization peak (SMP) and the associated pinning properties in a single crystal of the iron-pnictide $Ca_{0.82}La_{0.18}Fe_{0.96}Ni_{0.04}As_2$ superconductor. In isothermal $M(H)$ measurements for $H \parallel c$-axis, the SMP was observed for the entire temperature range below T_c. However, the SMP was observed only for temperatures close to T_c for $H \parallel ab$-planes. A detailed investigation based on Maley's analysis and collective pinning theory suggests that the SMP in the sample may be explained in terms of an elastic pinning to plastic pinning crossover across $H_{\rm p}$, which also seems accompanied with a possible vortex lattice phase transition. However, any direct observation of such phase transition in vortex lattice near $H_{\rm p}$ and its correlation with SMP is yet to be confirmed. For $H \parallel ab$-planes, the suppression of the SMP at low temperature may be related to the sample anisotropy, which in turn leads to the 2D Josephson vortices at low temperature and high magnetic fields. Based on the Dew-Hughes model, pinning analysis for $H \parallel c$ suggests that point disorder in addition with surface defects are the possible sources of vortex pinning, which are in favor of a δl-type pinning in the sample. Moreover, the critical current density has been found to be higher than 10^5 A cm^{-2} for temperatures below 8 K in the entire magnetic field range of the measurements. This property makes this compound technologically relevant for use in high magnetic field generation.

Data availability statement

All data that support the findings of this study are included within the article (and any supplementary files).

Acknowledgments

IFL, DS, and JM acknowledge support by the Spanish Agencia Estatal de Investigación (AEI) and Fondo Europeo de Desarrollo Regional (FEDER) through Project PID2019-104296GB-I00, and by Xunta de Galicia (Grant GRC No. ED431C 2018/11). IFL acknowledges financial support from Xunta de Galicia through Grant ED481A-2020/149. Authors would like to thank the use of RIAIDT-USC analytical facilities. SSS acknowledges support from CNPq and CAPES. This work at IOP, CAS is supported by the National Key Research and Development Program of China (Grants Nos. 2018YFA0704200, 2017YFA0303100, and 2017YFA0302900), the National Natural Science Foundation of China (Grants Nos. 11822411, 11961160699, and 11874401), the Strategic Priority Research Program (B) of the Chinese Academy of Sciences (CAS) (Grants Nos. XDB25000000 and XDB07020300) and K. C. Wong Education Foundation (GJTD-2020-01). HL is grateful for the support from the Youth Innovation Promotion Association of CAS (Grant No. Y202001).

ORCID iDs

I F Llovo https://orcid.org/0000-0002-8413-0034
J Mosqueira https://orcid.org/0000-0002-8639-2329
Shyam Sundar https://orcid.org/0000-0003-2855-7989
S-L Li https://orcid.org/0000-0001-7922-3730

References

[1] Hosono H, Yamamoto A, Hiramatsu H and Ma Y 2018 *Mater. Today* **21** 278
[2] Kwok W K, Welp U, Glatz A, Koshelev A E, Kihlstrom K J and Crabtree G W 2016 *Rep. Prog. Phys.* **79** 116501
[3] Lortz R, Musolino N, Wang Y, Junod A and Toyota N 2007 *Phys. Rev.* B **75** 094503
[4] Stamopoulos D, Speliotis A and Niarchos D 2004 *Supercond. Sci. Technol.* **17** 1261
[5] Rosenstein B, Shapiro B Y, Shapiro I, Bruckental Y, Shaulov A and Yeshurun Y 2005 *Phys. Rev.* B **72** 144512
[6] Salem-Sugui Jr S, Lopes P V, Kern M P, Sundar S, Liu S, Li S and Ghivelder H L L 2020 *Phys. Rev.* B **102** 064509
[7] Cheng W, Lin H, Shen B and Wen H H 2019 *Sci. Bull.* **64** 81
[8] Song D, Ishida S, Iyo A, Nakajima M, ichi Shimoyama J, Eisterer M and Eisaki H 2016 *Sci. Rep.* **6** 26671
[9] Wang C, Yi X, Sun X, Tang Q, Qiu Y, Luo Y and Yu B 2017 *Supercond. Sci. Technol.* **30** 085004
[10] Jung S G, Shin S, Jang H, Mikheenko P, Johansen T H and Park T 2017 *Supercond. Sci. Technol.* **30** 085009
[11] Sundar S, Salem-Sugui Jr S S, Alvarenga A D, Doria M M, Gu Y, Li S, Luo H and Ghivelder L 2019 *J. Appl. Phys.* **125** 123902
[12] Rosenstein B and Li D 2010 *Rev. Mod. Phys.* **82** 109
[13] Wang C *et al* 2021 *Supercond. Sci. Technol.* **34** 055001
[14] Kamihara Y, Watanabe T, Hirano M and Hosono H 2008 *J. Am. Chem. Soc.* **130** 3296
[15] Shen B, Cheng P, Wang Z, Fang L, Ren C, Shan L and Wen H H 2010 *Phys. Rev.* B **81** 014503
[16] Sundar S, Mosqueira J, Alvarenga A D, Sóñora D, Sefat A S and Salem-Sugui Jr S S 2017 *Supercond. Sci. Technol.* **30** 125007
[17] Sundar S, Jr S S S, Amorim H S, Wen H H, Yates K A, Cohen L F and Ghivelder L 2017 *Phys. Rev.* B **95** 134509
[18] Sundar S, Salem-Sugui Jr S S, Lovell E, Vanstone A, Cohen L F, Gong D, Lu R Z X, Luo H and Ghivelder L 2019 *ACS Appl. Electron. Mater.* **1** 179
[19] Salem-Sugui Jr S *et al* 2010 *Phys. Rev.* B **82** 054513
[20] Ahmad D, Choi W J, Seo Y I, Jung S G, Kim Y C, Salem-Sugui Jr S, Park T and Kwon Y S 2017 *Supercond. Sci. Technol.* **30** 105006
[21] Zhou W, Xing X, Wu W, Zhao H and Shi Z 2016 *Sci. Rep.* **6** 22278
[22] Galluzzi A, Buchkov K, Nazarova E, Tomov V, Grimaldi G, Leo A, Pace S and Polichetti M 2019 *Nanotechnology* **30** 254001
[23] Kopeliansky R, Shaulov A, Shapiro B Y, Yeshurun Y, Rosenstein B, Tu J J, Li L J, Cao G H and Xu Z A 2010 *Phys. Rev.* B **81** 092504
[24] Pramanik A K, Harnagea L, Nacke C, Wolter A U B, Wurmehl S, Kataev V and Büchner B 2011 *Phys. Rev.* B **83** 094502
[25] Salem-Sugui Jr S, Mosqueira J, Alvarenga A D, Sóñora D, Herculano E P, Hu D, Chen G and Luo H 2015 *Supercond. Sci. Technol.* **28** 055017
[26] Miu L, Ionescu A M, Miu D, Burdusel M, Badica P, Batalu D and Crisan A 2020 *Sci. Rep.* **10** 17274
[27] Zehetmayer M 2015 *Sci. Rep.* **5** 9244
[28] Miu D, Noji T, Adachi T, Koike Y and Miu L 2012 *Supercond. Sci. Technol.* **25** 115009
[29] Ionescu A M, Miu D, Crisan A and Miu L 2018 *J. Supercond. Nov. Magn.* **31** 2329
[30] Yakita H *et al* 2014 *J. Am. Chem. Soc.* **136** 846
[31] Zhou W, Zhuang J, Yuan F, Li X, Xing X, Sun Y and Shi Z 2014 *App. Phys. Express* **7** 063102
[32] Xing X, Zhou W, Zhou N, Yuan F, Pan Y, Zhao H, Xu X and Shi Z 2016 *Supercond. Sci. Technol.* **29** 055005
[33] Sóñora D, Carballeira C, Ponte J J, Xie T, Luo H, Li S and Mosqueira J 2017 *Phys. Rev.* B **96** 014516
[34] Weyeneth S *et al* 2009 *J. Supercond. Nov. Magn.* **22** 325
[35] Prozorov R, Tillman M E, Mun E D and Canfield P C 2009 *New J. Phys.* **11** 035004
[36] Xie T *et al* 2017 *Supercond. Sci. Technol.* **30** 095002
[37] Salem-Sugui Jr S, Ghivelder L, Alvarenga A D, Cohen L F, Luo H and Lu X 2011 *Phys. Rev.* B **84** 052510
[38] Salem-Sugui Jr S, Ghivelder L, Alvarenga A D, Cohen L F, Luo H and Lu X 2013 *Supercond. Sci. Technol.* **26** 025006
[39] Sharma S, Vinod K, Sundar C S and Bharathi A 2013 *Supercond. Sci. Technol.* **26** 015009
[40] Moll P J W, Balicas L, Geshkenbein V, Blatter G, Karpinski J, Zhigadlo N D and Batlogg B 2012 *Nat. Mater.* **12** 134
[41] Beasley M R, Labusch R and Webb W W 1969 *Phys. Rev.* **181** 682 references therein
[42] Feigel'man M V, Geshkenbein V B, Larkin A I and Vinokur V M 1989 *Phys. Rev. Lett.* **63** 2303
[43] Maley M P, Willis J O, Lessure H and McHenry M E 1990 *Phys. Rev.* B **42** 2639(R)
[44] McHenry M E, Simizu S, Lessure H, Maley M P, Coulter J Y, Tanaka I and Kojima H 1991 *Phys. Rev.* B **44** 7614
[45] Abulafia Y *et al* 1996 *Phys. Rev. Lett.* **77** 1596
[46] Fehrenbacher R, Geshkenbein V B and Blatter G 1992 *Phys. Rev.* B **45** 5450
[47] Polichetti M, Galluzzi A, Buchkov K, Tomov V, Nazarova E, Leo A, Grimaldi G and Pace S 2021 *Sci. Rep.* **11** 7247
[48] Bean C P 1962 *Phys. Rev. Lett.* **8** 250
[49] Poole C, Farach H, Creswick R and Prozorov R 2007 *Superconductivity* (New York: Academic)
[50] Yeshurun Y and Malozemoff A P 1988 *Phys. Rev. Lett.* **60** 2202
[51] Galluzzi A, Buchkov K, Tomov V, Nazarova E, Leo A, Grimaldi G, Nigro A, Pace S and Polichetti M 2018 *Supercond. Sci. Technol.* **31** 015014
[52] Rosenstein B and Zhuravlev V 2007 *Phys. Rev.* B **76** 014507
[53] Prozorov R *et al* 2008 *Phys. Rev.* B **78** 224506
[54] Deligiannis K, de Groot P A J, Oussena M, Pinfold S, Langan R, Gagnon R and Taillefer L 1997 *Phys. Rev. Lett.* **79** 2121
[55] Griessen R, Wen H H, van Dalen A J J, Dam B, Rector J and Schnack H G 1994 *Phys. Rev. Lett.* **72** 1910
[56] Galluzzi A, Buchkov K, Tomov V, Nazarova E, Leo A, Grimaldi G, Nigro A, Pace S and Polichetti M 2019 *J. Phys.: Conf. Ser.* **1226** 012012
[57] Dew-Hughes D 1974 *Phil. Mag.* **30** 293
[58] Koblischka M R and Muralidhar M 2016 *Int. J. Mod. Phys.* B **30** 1630017
[59] Zhang Q, Zhang X, Yao C, Huang H, Wang D, Dong C, Ma Y, Ogino H and Awaji S 2017 *Superc. Sci. Technol.* **30** 065004
[60] Shahbazi M, Wang X L, Dou S X, Fang H and Lin C T 2013 *J. Appl. Phys.* **113** 17E115
[61] Shahbazi M, Wang X L, Choi K Y and Dou S X 2013 *Appl. Phys. Lett.* **103** 032605
[62] Gennep D V, Hassan A, Luo H and Abdel-Hafiez M 2020 *Phys. Rev.* B **101** 235163